

# TANDEM-X: A SATELLITE FORMATION FOR HIGH RESOLUTION SAR INTERFEROMETRY

Gerhard Krieger, Alberto Moreira, Hauke Fiedler, Irena Hajnsek, Michael Eineder, Manfred Zink, Marian Werner

*Microwaves and Radar Institute, German Aerospace Centre (DLR), 82234 Oberpfaffenhofen, Germany  
E-Mail: Gerhard.Krieger@dlr.de*

## ABSTRACT

TanDEM-X is a mission proposal for an innovative spaceborne radar interferometer which has been evaluated in a phase A study by a joint DLR and EADS/Astrium team. The mission concept is based on two TerraSAR-X radar satellites flying in close formation to achieve the desired interferometric baselines in a highly reconfigurable configuration. The main goal of the TanDEM-X mission is the generation of a world-wide, consistent, timely, and high-precision digital elevation model according to the HRTI/DTED-3 standard as the basis for a wide range of scientific research, as well as for operational, commercial DEM production. Secondary mission goals of TanDEM-X are moving target indication with a distributed four aperture displaced phase centre system, the measurement of ocean currents and the detection of ice drift by along-track interferometry, high resolution SAR imaging based on a baseline induced shift of the Doppler and range spectra (super-resolution), the derivation of vegetation parameters with polarimetric SAR interferometry, large baseline bistatic SAR imaging for improved scene classification, as well as regional very high resolution DEM generation based on spotlight and large baseline interferometry. The feasibility of these modes will be investigated and predictions about the achievable performance will be made.

## I. INTRODUCTION

Digital elevations models (DEMs) are of fundamental importance for a broad range of commercial and scientific applications. For example, many geoscience areas like hydrology, glaciology, forestry, geology, oceanography and land environment require precise and up-to-date information about the Earth's surface and its topography. Digital maps are also a prerequisite for reliable navigation, and improvements in their precision needs to keep step with the advances in global positioning systems, like GPS and Galileo. In principle, DEMs can be derived from a variety of spaceborne sensors. However, the resulting mosaic of data from different sources with a multitude of horizontal and vertical data, accuracies, formats, map projections, time differences and resolutions is hardly a uniform and reliable data set. The Shuttle Radar Topography Mission (SRTM) had hence the challenging goal to meet the requirements for a homogeneous and reliable DEM fulfilling the DTED-2 specification (cf. third column of Table 1). However, many scientific and commercial applications require improved accuracy, corresponding to the emerging HRTI/DTED-3 standard (12 m posting and 2 m height accuracy, cf. right column of Table 1) and comparable to DEMs generated by high-resolution airborne SAR systems [1][2][3].

TABLE I. Comparison of DTED2 and HRTI-3 DEM Specifications

| Requirement                | Specification                   | DTED-2                                   | HRTI-3                                 |
|----------------------------|---------------------------------|------------------------------------------|----------------------------------------|
| Relative Vertical Accuracy | 90% linear point-to-point error | 12 m (slope < 20%)<br>15 m (slope > 20%) | 2 m (slope < 20%)<br>4 m (slope > 20%) |
| Absolute Vertical Accuracy | 90% linear error                | 18 m                                     | 10 m                                   |
| Horizontal Accuracy        | 90% circular error              | 23 m                                     | 10 m                                   |
| Spatial Resolution         | independent pixels              | 30 m (1 arc sec)                         | 12 m (0.4 arc sec)                     |

This paper describes the TanDEM-X mission concept and requirements, including several innovative aspects like operation modes, orbit selection and maintenance as well as phase synchronization. Results from a detailed performance estimation show the achievable DEM accuracy. Finally, an overview of the potential of the TanDEM-X mission for several scientific applications is presented.

## II. MISSION CONCEPT

The TanDEM-X mission concept is based on an extension of the TerraSAR-X mission [4] by a second TerraSAR-X like satellite (TanDEM-X). Both satellites will fly in a close orbit formation and will be operated as a flexible single-pass SAR interferometer, where the baseline can be selected according to the specific needs of the application (cf. Figure 1). This enables the acquisition of highly accurate cross-track and along-track interferograms without the inherent accuracy limitations imposed by repeat-pass interferometry due to temporal decorrelation and atmospheric disturbances [5].

The TanDEM-X satellite (TDX) will be designed for a nominal lifetime of 5 years and has a nominal overlap with TerraSAR-X (TSX-1) of 3 years. A prolongation of the mission overlap is possible by means of an extension of TSX-1 operation which is compatible with the TSX-1 consumables and resources.

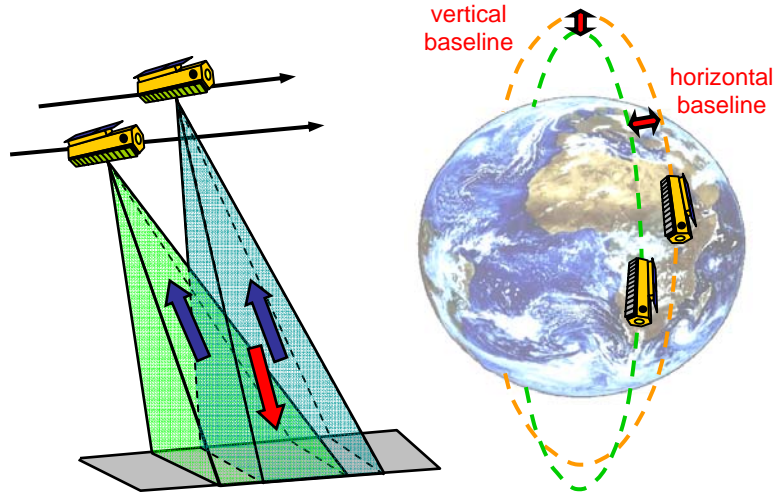


Figure 1: Bistatic InSAR Operation (left) and HELIX [7] orbit (right).

Interferometric data acquisition can be performed in (1) the pursuit monostatic mode where both satellites are operated independently, (2) the bistatic mode where one satellite serves as a transmitter and both satellites record the scattered signal simultaneously, and (3) the alternating bistatic mode where the transmitter changes from pulse to pulse. Current baseline for operational DEM generation is the bistatic mode which minimizes temporal decorrelation and makes efficient use of the transmit power. The alternating bistatic mode can be used for phase synchronization, system calibration, and to acquire interferograms with two different phase-to-height sensitivities, but the simultaneously acquired monostatic interferogram has a higher susceptibility to ambiguities especially at high incident angles [6]. Monostatic data takes are planned during the commissioning phase and at the end of the mission where the satellite formation is flown with a sufficient along-track separation between the satellites to avoid potential RF interferences.

The TanDEM-X operational scenario requires a coordinated operation of two satellites flying in close formation. Several options have been investigated and the HELIX satellite formation has finally been selected. This formation combines an out-of-plane orbital displacement (e.g. by different ascending nodes) with a radial (vertical) separation (e.g. by different eccentricity vectors) resulting in a helix like relative movement of the satellites along the orbit [7]. Since there exists no crossing of the satellite orbits, it is now possible to arbitrarily shift the satellites along their orbits, e.g. to adjust very small along-track baselines at predefined latitudes [8] and to allow safe spacecraft operation without autonomous control [9]. The HELIX formation enables a complete coverage of the Earth with a stable height of ambiguity by using a small number of formations (e.g.  $a\Delta\Omega=\{300\text{m},400\text{m},500\text{m}\}$  and  $a\Delta e=\{300\text{m},500\text{m}\}$ , [10]). Baseline fine tuning can be achieved by taking advantage of the natural rotation of the eccentricity vectors due to secular disturbances and fixating the eccentricity vectors at different relative phasings. An appropriate reference scenario has been derived which enables one complete coverage of the Earth with baselines corresponding to a height of ambiguity of ca. 35m (see Sect. III) within somewhat more than 1 year assuming a bistatic acquisition in strip map mode with an average acquisition time of 140s per orbit [10].

### III. PERFORMANCE ANALYSIS

This section investigates the interferometric performance of TanDEM-X. For this, an interferometric data acquisition in bistatic strip map mode will be assumed. Table 1 summarizes the main instrument, orbit, and processing parameters which have been used in the performance analysis.

TABLE II. TanDEM-X System Parameters

| Parameter                                 | Value          | Parameter                               | Value             |
|-------------------------------------------|----------------|-----------------------------------------|-------------------|
| Satellite Height (nom.)                   | 514 km         | Antenna Length                          | 4,8 m             |
| Nominal Swath Width                       | 30 km          | Antenna Width                           | 0,7 m             |
| Swath Overlap                             | 6 km           | Antenna Elements                        | 32 x 12           |
| Carrier Frequency                         | 9,65 GHz       | Antenna Tapering                        | linear phase      |
| Chirp Bandwidth                           | $\leq 150$ MHz | Antenna Mounting                        | 33,8°             |
| Peak Tx Power                             | 2260 W         | Quantization                            | 4 bits/sample     |
| Duty Cycle                                | 18 %           | Proc. Az. Bandwidth                     | 2266 Hz           |
| Noise Figure TRM                          | 4.3 dB         | Misregistration                         | 0.1 pixel         |
| Losses (proc., atm., taper, degrad., ...) | 4.1 dB         | Sigma Nought Model (Ulaby, 90%, X-band) | Soil and Rock, VV |
| Indep. Post Spacing                       | 12 m x 12 m    | Along-Track Baseline                    | < 1 km            |

### A. Relative Height Accuracy

Major factors which affect the relative height accuracy are the radiometric sensitivity of each SAR instrument, range and azimuth ambiguities, quantization noise, processing and co-registration errors as well as surface and volume decorrelation, scaled by the baseline length [11]. For the performance estimation, the chirp bandwidth has been selected to yield a constant ground range resolution of 3 m and no antenna tapering was used to compensate for the steep sensitivity decay at the swath borders. Future TanDEM-X system optimizations could include an appropriate Rx elevation tapering as well as a complete redefinition of the beams to improve both the sensitivity and the coverage by using optimized beams with less overlap. The total coherence has been computed by the product

$$\tilde{\gamma}_{tot} = \gamma_{SNR} \cdot \gamma_{Quant} \cdot \gamma_{Amb} \cdot \gamma_{Coreg} \cdot \gamma_{Geo} \cdot \gamma_{Az} \cdot \tilde{\gamma}_{Vol} \cdot \tilde{\gamma}_{Temp} \quad (1)$$

where the right hand side describes the different error contributions due to the limited SNR, quantization, ambiguities, limited coregistration accuracy, etc. (cf. [12]). The contribution from each of these terms has been evaluated for TanDEM-X and Figure 2 shows the predicted total coherence assuming the 50% (dotted) and 90% (solid) occurrence levels of the scattering coefficients.

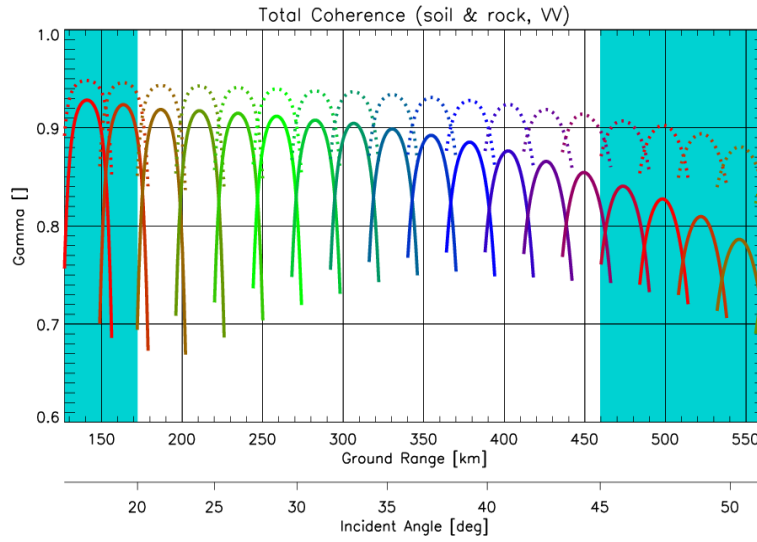


Figure 2: Total coherence in strip map mode.

In order to calculate the height accuracy, the interferometric phase errors have first been estimated from the total coherence taking into account the number of independent looks obtained after spectral filtering in range and azimuth. Figure 2 shows the predicted height accuracy for an effective baseline of 600m assuming an operation of TanDEM-X in bistatic strip map mode. The solid lines indicate point-to-point height errors for a 90% confidence interval, and the dotted lines indicate the corresponding standard deviation. The height errors in Figure 2 show a significant increase from near range to far range swaths. One reason for this increase is the systematic decrease of the phase to height scaling corresponding to a systematic increase of the height of ambiguity with increasing incident angles.

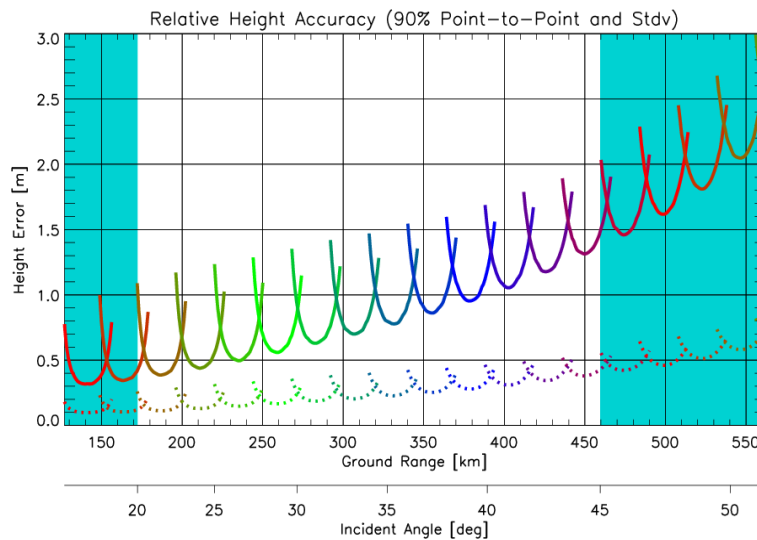


Figure 3: Relative height accuracy for an effective baseline of 600 m in strip map mode. (solid: point-to-point height errors for a 90% confidence interval, dotted: standard deviation)

As TanDEM-X enables a flexible selection of the interferometric baseline, it is hence advisable to adapt the length of the baselines to a fixed minimum height of ambiguity. As an example, Figure 4 shows the point-to-point height errors for the 90% confidence interval assuming fixed heights of ambiguity of 50m (top), 35m (middle), and 20m (bottom). Note that the derivation of the height accuracy assumes a maximum likelihood combination of the interferometric data from overlapping swath segments. The impacts of slopes, volume decorrelation, etc. have been analysed in [6], where it is shown that e.g. a variation of the slopes by  $\pm 20\%$  may cause a maximum increase of the height errors by a factor of  $< 1.1$  for medium incident angles and 1.2 for either very steep or very shallow incident angles.

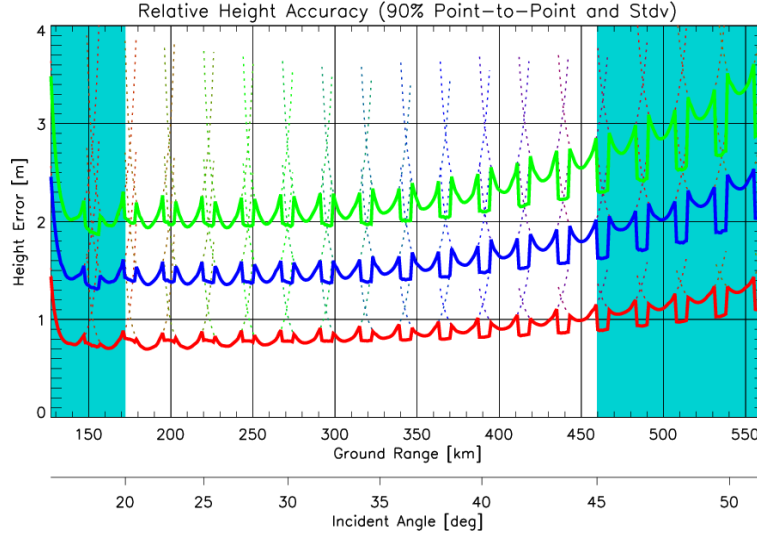


Figure 4: Height accuracy for fixed heights of ambiguity of 50m (top, green), 35m (middle, blue) and 20m (bottom, red) in strip map mode after combining adjacent swaths. Shown are point-to-point height errors for a 90% confidence interval.

It becomes apparent from Figure 4 that the acquisition of DEMs with 2m relative height accuracy (point-to-point errors at 90% occurrence level according to HRTI-3 standard) will require a height of ambiguity which is in the order of 35m. This height of ambiguity corresponds to perpendicular baselines of  $B_{\perp}=260\text{m}$  and  $B_{\perp}=439\text{m}$  at incident angles of  $30^{\circ}$  and  $45^{\circ}$ , respectively. It is clear, that unambiguous DEM generation in mountainous areas will require additional data acquisitions with different baselines to support phase unwrapping as described in [13] by, e.g., employing an appropriate adaptation of the maximum likelihood technique suggested in [14]. The current TanDEM-X mission concept assumes 1-2 additional data acquisitions for areas with moderate slopes and tall vegetation and 3-4 additional acquisitions for mountainous terrain with steep slopes. Phase unwrapping in forested areas may also be improved by evaluating the coherence loss due to volume decorrelation. Difficult terrain can furthermore be imaged with smaller baselines in the alternating bistatic mode, which enables the acquisition of two interferograms with an effective baseline ratio of two in one single pass.

## B. Baseline Estimation Errors

Up to now, we have neglected errors due to the finite accuracy of relative baseline estimation and relative RF phase knowledge. Such errors will mainly cause a low frequency modulation of the DEM, thereby contributing simultaneously to relative and absolute height errors. For the latter, the HRTI-3 standard is much less stringent and requires an accuracy of 10m at a 90% confidence level.

Baseline estimation errors can be divided into along-track, cross-track, and radial errors. Along-track errors will be sufficiently resolved during the co-registration and are hence regarded as uncritical. Cross-track and radial errors may cause errors in both the line of sight ( $\Delta B_{||}$ ) and perpendicular ( $\Delta B_{\perp}$ ) to the line of sight. Baseline errors perpendicular to the line of sight will cause a bias in the phase to height scaling. The resulting height error is given by  $\Delta h = h \cdot \Delta B_{\perp} / B_{\perp}$ , where  $h$  is the topographic height,  $\Delta B_{\perp}$  is the error of the baseline estimate perpendicular to the line of sight, and  $B_{\perp}$  is the length of the perpendicular baseline. Assuming a maximum topographic height of  $h=9000\text{m}$  and baselines corresponding to a height of ambiguity of  $h_{\text{amb}}=35\text{m}$  (i.e.  $B_{\perp}=260\text{m}$  for  $\theta_i=30^{\circ}$  and  $B_{\perp}=439\text{m}$  for  $\theta_i=45^{\circ}$ ), a baseline estimation error of  $\Delta B_{\perp}=\pm 1\text{mm}$  will result in height errors of  $\pm 3.5\text{cm}$  and  $\pm 2.1\text{cm}$  for incident angles of  $\theta_i=30^{\circ}$  and  $\theta_i=45^{\circ}$ , respectively.

Errors in the relative position estimates of the antenna phase centres parallel to the line of sight ( $\Delta B_{||}$ ) will primarily cause a rotation of the reconstructed DEM about the (master) satellite position. As a result, the DEM will be vertically displaced by  $\Delta h = \Delta B_{||} / B_{\perp} \cdot r \cdot \sin(\theta_i) = \Delta B_{||} \cdot h_{\text{amb}} / \lambda$  where  $r$  and  $\theta_i$  are the slant range distance and the incident angle of an appropriately selected reference point (e.g. at mid swath). This vertical displacement will be  $\Delta h = \pm 1.1\text{m}$  for  $\Delta B_{||} = \pm 1\text{mm}$  and  $h_{\text{amb}} = 35\text{m}$ . A parallel baseline error of one satellite will furthermore cause a tilt of the DEM which is given by  $\phi_{\text{tilt}} = \Delta h / \Delta s = \Delta B_{||} / B_{\perp}$  where  $\Delta s$  is the ground range distance from the selected reference point. The resulting tilt will be  $3.8\text{mm/km}$  and  $2.3\text{mm/km}$  for incident angles of  $\theta_i=30^{\circ}$  and

$\theta_i=45^\circ$ , respectively ( $\Delta B_{||}=1\text{mm}$  and  $h_{\text{amb}}=35\text{m}$ ). Table 4 summarizes the predicted height errors resulting from  $\Delta B_{||}=1\text{mm}$  and  $\Delta B_{\perp}=1\text{mm}$ .

TABLE III. Height Errors for 1mm Baseline Estimation Uncertainty

| Incident Angle | Normal Baseline ( $h_{\text{amb}}=35\text{m}$ ) | Height Errors (for $h_{\text{amb}}=35\text{m}$ ) |                            |                                 |
|----------------|-------------------------------------------------|--------------------------------------------------|----------------------------|---------------------------------|
|                |                                                 | $\Delta B_{  } = 1\text{mm}$                     |                            | $\Delta B_{\perp} = 1\text{mm}$ |
|                |                                                 | $\Delta h$                                       | $\Delta h/\Delta s$ (tilt) | $\Delta h$ ( $h=9\text{km}$ )   |
| $30^\circ$     | 260 m                                           | 1.1 m                                            | 3.8 mm/km                  | 3.5 cm                          |
| $45^\circ$     | 439 m                                           |                                                  | 2.3 mm/km                  | 2.1 cm                          |

The current mission concept assumes precise baseline determination by a direct evaluation of GPS carrier phase measurements. Current analyses indicate an achievable accuracy for the estimation of relative satellite positions in the order of 1-2mm [15]. The additional impact of satellite attitude errors and uncertainties in both the GPS and the RF antenna phase centre positions are currently being investigated. Note in this context that both satellites experience almost the same gravity field and are exposed to highly correlated orbital perturbations. Residual (i.e. unmodelled) variations of the baseline vector will hence show a high degree of temporal correlation. Even in case of a large differential acceleration of  $a=100*10^{-9}\text{m/s}^2$  (e.g. due to unmodelled differential drag between the two satellites, etc.), the resulting differential error after a 100km data take will be in the order of only  $10\mu\text{m}$ . Noting furthermore, that such an acceleration will mainly affect estimates of the along-track baseline (which are uncritical for cross-track interferometry), we may conclude that residual orbit fluctuations can be neglected in the computation of relative height errors (the area for relative point-to-point height errors in HRTI-3 is  $100\text{km} \times 100\text{km}$ ).

Not neglected for the computation of relative height errors can, however, be the DEM tilt resulting from initial estimation errors of the relative RF antenna phase centre position. For example, an initial error in the estimate of the RF relative phase centre position of  $\Delta B_{||}=\pm 1\text{cm}$  can in the worst case result in a relative height error of  $\pm 3.8\text{m}$  for  $\Delta s=100\text{km}$  (assuming an ideal mosaicking of equally tilted swaths). Such a tilt can be reduced by additional calibration data takes from crossing orbits by applying an appropriate bundle block adjustment in either radar or DEM geometry. Calibration data takes could also profit from larger baselines and/or different interferometric (e.g. pursuit monostatic or alternating bistatic) and/or different SAR (e.g. ScanSAR) modes. Absolute DEM calibration requires a final height accuracy of 10m and will be based on a combination of (1) a sparse net of calibration targets, (2) GPS tracks, and (3) ocean data takes with short along-track baselines. Further calibration strategies are currently under investigation.

### C. Oscillator Phase Errors

The impact of oscillator phase noise in bistatic mode has been analyzed in [16] where it is shown that oscillator noise may cause errors in both the interferometric phase and SAR focusing. Such errors can be estimated from a linear systems model that weights the power spectral density of the oscillator phase noise. The stringent requirements for interferometric phase stability in the bistatic mode will require an appropriate relative phase referencing or an operation in the alternating bistatic mode. Direct transmission and reception of radar pulses is foreseen on both the TerraSAR-X and the TanDEM-X satellites. Assuming a height of ambiguity of 35m, the sensitivity to phase errors will be  $h_{\text{amb}}/360^\circ=0.097\text{m/deg}$ . The maximum allowed phase error for a height error of  $\pm 1\text{m}$  is hence  $\pm 10.3^\circ$ . The required update frequency in the direct transmission mode is in the order of 1-10Hz depending on (1) the tolerable height errors, (2) the exact specification of the phase spectra of the two local oscillators, and (3) the phase noise on the 'synchronisation' link [16].

## IV. SCIENTIFIC APPLICATIONS

TanDEM-X has been designed to provide high quality data for commercial and scientific applications [17]. As far as the scientific applications and corresponding geo-physical products are concerned, they have been endorsed with a questionnaire distributed to approx. 100 international scientists [18]. Many of the scientists represent end-users and have a long experience with the SRTM, SIR-C/X-SAR as well as ERS-1/2 data evaluation. The scientific applications can be summarized in three groups:

### A. Across-Track Interferometry

A consistent and reliable DEM data set with global coverage and HRTI/DTED-3 standard provides important information for a variety of on-going research areas and will allow new scientific applications to be developed. Examples are:

- *Hydrology* (ice and snow, wetlands, morphology and flooding),
- *Geology* (geological mapping, tectonics, volcanoes and land-slides),
- *Land Environment* (cartography, urban areas, disaster and crisis management, navigation, archaeology and change detection),
- *Renewable Resources* (land use mapping, agriculture, forestry and grassland),
- *Oceanography* (wind and waves, ocean dynamics, sea-ice, ship detection, oil slicks and bathymetry).

Some of these applications foresee the combined use of along- and across-track interferometry as well as polarimetry to enhance current products. Further promising applications result from the acquisition of cross-track interferograms with huge interferometric baselines. Such acquisitions take advantage from the large bandwidth of TerraSAR-X and it becomes possible to significantly improve the height accuracy for local areas by combining multiple interferograms with different baseline lengths. Multi-temporal large baseline TanDEM-X interferograms are furthermore well suited to detect and measure vertical changes on a decimeter level.

### B. Along-Track Interferometry

Along-track interferometry will allow innovative applications to be explored. Along-track interferometry can be performed by the so-called dual-receive antenna mode in each of the two tandem satellites (ca. 2.4 m along-track baseline, cf. [19]) and/or by adjusting the along-track distance between TSX-1 and TDX to the desired value. The combination of both modes will provide a highly capable along-track interferometer with four phase centers. As outlined in Section II, the along-track component can be adjusted from zero to several kilometers. The combination of the different along-track baselines will e.g. be used for improved detection, localisation and ambiguity resolution in ground moving target indication (GMTI) and traffic monitoring applications. The following sub-groups have been defined for along-track interferometry:

- *Oceanography* (Ocean currents maps, ocean wave spectra),
- *Moving Target Detection* (Traffic flow monitoring maps, see also moving target techniques in application area IV.C),
- *Glaciology* (Ice drift and Ice flow monitoring maps).

### C. New Techniques with Bi-Static SAR

The TanDEM-X mission will provide the remote sensing scientific community with a unique data set to exploit the capability of new bi-static radar techniques and to apply these innovative techniques for enhanced parameter retrieval [20]. Examples are:

- *Super Resolution* (high resolution maps, micro-topography enhancement maps, feature extraction algorithms),
- *Bi-static SAR* (new bi-static SAR processing algorithms, multi-angle SAR, enhanced scene feature extraction, combination of mono-static and bi-static signatures),
- *Moving Target Indication* (detection of ground moving targets and the estimation of their velocity, moving target relocation, isolation and target focusing),
- *Polarimetric SAR Interferometry* (DEM optimization using polarization diversity, vegetation bias and structure maps, crop biomass). Figure 5 illustrates the achievable performance (see also [12]). This analysis is based on the Random Volume over Ground (RVoG) model [21] assuming a vegetation layer with a height of 0,6 m and an extinction coefficient of 10 dB/m. The dashed line indicates the height variation of the interferometric phase centre with different polarisations (corresponding to a variation of  $\mu$  on the abscissa). The green tube shows the height errors due to volume decorrelation for an effective baseline of 5 km and an independent post-spacing of 30m x 30m. The blue tube shows additional errors due to the limited system accuracy and the red tube indicates potential errors in case of temporal decorrelation caused by a possible along-track separation between the two satellites (here:  $\gamma_{tmp} = 0.7$ ). The performance analysis predicts a sufficient phase centre separation to enable a successful retrieval of important vegetation parameters like volume height, extinction, etc.

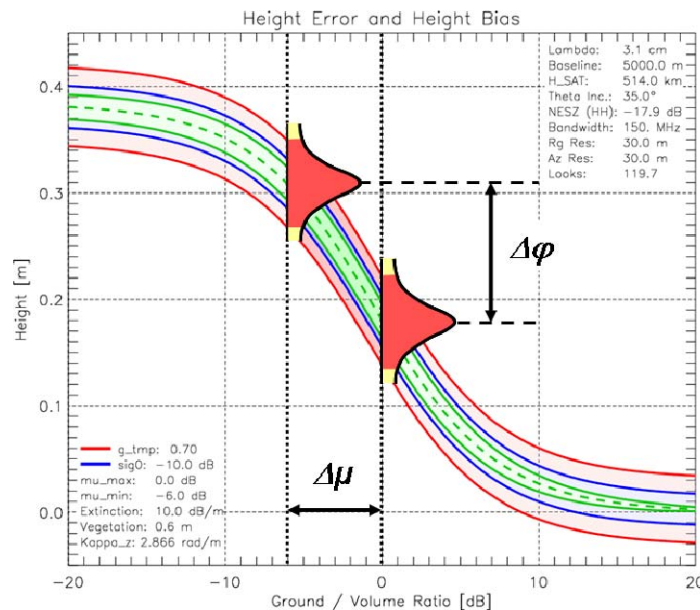


Figure 5: Vertical separation of interferometric phase centres in TanDEM-X as a function of the ground-to-volume scattering ratios  $\mu$  (cf. [12])

## V. CONCLUSION

The phase A study of TanDEM-X has been completed in June 2005. The feasibility of the mission and of associated key technologies has been demonstrated:

- global scale, operational DEM generation with an accuracy corresponding to the HRTI-3 standard,
- close formation flying to ensure suitable baselines for interferometric processing,
- baseline determination capability down to a few millimeters,
- phase and time synchronization of the tandem instrument configuration.

The achievable height accuracy in TanDEM-X is mainly limited by the height of ambiguity that can finally be processed during phase unwrapping. A mission concept has been developed which enables the acquisition of a global DEM within three years. This concept includes several data takes with different baselines, different incident angles, and data takes from ascending and descending orbits to deal with difficult terrain like mountains, valleys, tall vegetation, etc.

The TanDEM-X mission concept allocates also sufficient acquisition time and satellite resources to secondary mission goals like moving target indication with a distributed four aperture displaced phase centre system, the measurement of ocean currents and the detection of ice drift by along-track interferometry, high resolution SAR imaging based on a baseline induced shift of the Doppler and range spectra (super-resolution), the derivation of vegetation parameters with polarimetric SAR interferometry, large baseline bistatic SAR imaging for improved scene classification, demonstration of high resolution wide swath SAR imaging with four phase centre digital beamforming, as well as localized very high resolution DEM generation based on spotlight and/or large baseline interferometry [1][2].

Current work includes an optimization of the mission scenario by redefining the standard TerraSAR-X beams to improve both the performance and the coverage, an in depth analysis of the synchronization link, the development of a detailed calibration plan, the development of a multibaseline processing concept, as well as performance investigations for the other TanDEM-X imaging modes.

## VI. REFERENCES

- [1] A. Moreira, G. Krieger, I. Hajnsek, M. Werner, D. Hounam, S. Riegger, E. Settemeyer, TanDEM-X: A TerraSAR-X Add-On Satellite for Single-Pass SAR Interferometry, IGARSS 2004, Anchorage, USA.
- [2] G. Krieger, A. Moreira, I. Hajnsek, D. Hounam, M. Werner, S. Riegger, E. Settemeyer, A Tandem TerraSAR-X Configuration for Single-Pass SAR Interferometry, Radar 2004, Toulouse (see also ISPRS WS, 2005).
- [3] I. Hajnsek, M. Weber, TanDEM-X: Science and Custom Exploration, IGARSS 2005, Seoul, Korea.
- [4] R. Werninghaus, W. Balzer, St. Buckreuss, J. Mittermayer, P. Mühlbauer, The TerraSAR-X Mission, EUSAR 2004, Ulm, Germany.
- [5] R. Hanssen, Radar Interferometry, Kluwer, Dordrecht, 2001.
- [6] G. Krieger, TanDEM-X Phase A Study: Preliminary Mission Analysis and System Performance, TSXT-RD-DLR-1100, January 2005.
- [7] A. Moreira, G. Krieger, J. Mittermayer, Satellite Configuration for Interferometric and/or Tomographic Remote Sensing by Means of Synthetic Aperture Radar (SAR), US Patent 6,677,884, July 2002. (see also Proc. Advanced SAR Workshop, Saint Hubert, Canada, 2001).
- [8] H. Fiedler, G. Krieger, Close Formation of Passive Receiving Micro-satellites, 18<sup>th</sup> Int. Symp. Space Flight Dynamics, Germany, 2004.
- [9] S. D'Amico, O. Montenbruck, C. Arbinger, H. Fiedler, Formation Flying Concept for Close Remote Sensing Satellites, AAS 05-156, 2005.
- [10] H. Fiedler, TanDEM-X Phase A Study: Development of a Reference Scenario for TanDEM-X, April 2005.
- [11] G. Krieger, H. Fiedler, J. Mittermayer, K. Papathanassiou, A. Moreira, Analysis of Multistatic Configurations for Spaceborne SAR Interferometry, IEE Proc. Radar, Sonar Navigation, Vol. 150, No. 3, pp. 87-96, 2003.
- [12] G. Krieger, K. Papathanassiou, S. Cloude, Spaceborne Polarimetric SAR Interferometry: Performance Analysis and Mission Concepts, EURASIP Journal on Applied Signal Processing, Vol. 20, pp. 3272-3292, 2005.
- [13] M. Eineder, G. Krieger, Interferometric Digital Elevation Model Reconstruction – Experiences from SRTM and Multi Channel Approaches for Future Missions, IGARSS 2005, Seoul, Korea.
- [14] M. Eineder, N. Adam, A maximum-likelihood estimator to simultaneously unwrap, geocode, and fuse SAR interferograms from different viewing geometries into one digital elevation model. IEEE Trans. Geosci. Remote Sens., Vol. 43, No. 1, pp. 24-36, 2005.
- [15] R. Kroes, O. Montenbruck, W. Bertiger, P. Visser, Precise GRACE baseline determination using GPS, GPS Solut, Vol. 9, pp. 21-31, 2005.
- [16] G. Krieger and M. Younis, Impact of Oscillator Noise in Bistatic and Multistatic SAR, IEEE Geoscience and Remote Sensing Letters, in revision, 2006.
- [17] A. Moreira et al.: TanDEM-X: TerraSAR-X Add-On for Digital Terrain Elevation Measurements, Mission Description Document No. 2003-3472739, Issue 1.2, 21 June 2005.
- [18] I. Hajnsek and M. Weber: TanDEM-X User Requirements Document, Technical Note TDX-RD-DLR-1201, Issue 1.2, 20 June 2005.
- [19] J. Mittermayer and H. Runge, Conceptual Studies for Exploiting the TerraSAR-X Dual Receive Antenna, IGARSS 2003, Toulouse, France.
- [20] G. Krieger and A. Moreira, Spaceborne Bistatic and Multistatic SAR: Potentials and Challenges, to appear in IEE Proc. Radar Sonar Navigation, 2006.
- [21] S.R. Cloude and K.P. Papathanassiou, A 3-Stage Inversion Process for Polarimetric SAR Interferometry, IEE Proc. Radar, Sonar Navigation, Vol. 150, No. 3, pp. 125-134, 2003.